Pump-induced carrier envelope offset frequency dynamics and stabilization of an Yb-doped fiber frequency comb*

Zhao Jian(赵 健), Li Wen-Xue(李文雪)†, Yang Kang-Wen(杨康文), Shen Xu-Ling(沈旭玲), Bai Dong-Bi(白东碧), Chen Xiu-Liang(陈修亮), and Zeng He-Ping(曾和平)

State Key Laboratory of Precision Spectroscopy, East China Normal University, Shanghai 200062, *China*

(Received 7 May 2014; revised manuscript received 30 June 2014; published online 10 October 2014)

In this paper, we demonstrate a carrier envelope phase-stabilized Yb-doped fiber frequency comb seeding by a nonlinear-polarization-evolution (NPE) mode-locked laser at a repetition rate of 60 MHz with a pulse duration of 191 fs. The pump-induced carrier envelope offset frequency (f_0) nonlinear tuning is discussed and further explained by the spectrum shift of the laser pulse. Through the environmental noise suppression, the drift of the free-running f_0 is reduced down to less than 3 MHz within an hour. By feedback control on the pump power with a self-made phase-lock loop (PLL) electronics the carrier envelope offset frequency is well phase-locked with a frequency jitter of 85 mHz within an hour.

Keywords: optical frequency comb, phase-locked loop, mode locking, fiber laser

PACS: 42.55.Wd, 06.60.Jn, 42.65.–k, 42.62.Eh **DOI:** 10.1088/1674-1056/23/12/124206

1. Introduction

Optical frequency combs have made significant progress on the precision metrology of time and frequency,[1,2] and been widely used as essential tools in optical clocks, precision atomic and molecular spectroscopy, ultralow noise microwave photonics, and calibration of astronomical spectrographs.[3] So far, most optical frequency combs are based on the mode-locked solid-state bulk or fiber lasers. Solid-state bulk lasers such as Ti:sapphire and Yb-doped crystal typically require critical bulk optical design and alignment.[4–6] Rare-earth-doped (such as Er^{3+}, Yb^{3+}, and Tm^{3+} dopants) fiber lasers are attractive since laser pulses are well-confined in the fiber waveguides so that they are extremely robust even under significant vibration.[7,8] In various existing technologies, the Yb-fiber frequency comb has attracted considerable interests for its low-cost direct diode pump, inherent robustness of fiber system, and suitability for high-power amplification.[9–11] Until now, the Yb-doped fiber frequency comb can reach an average power up to 100 W,[12] which makes it feasible to realize a phase coherent extreme ultraviolet (XUV) source with photon energy of 100 eV.[13] Besides, the second or fourth harmonics[12,14] are spectrally overlapped with some important narrow linewidth optical transitions, such as Al^+ (267 nm), Hg^+ (281.5 nm), and Yb (578.4 nm), which are excellent candidates for the next-generation frequency standard.[15]

The Yb-doped fiber frequency comb could be mode-locked by using saturable absorber, nonlinear optical loop mirror (NOLM) or nonlinear-polarization-evolution (NPE) effect.[16–18] Although mode-locking initiated by saturable absorber can be quite stable, special absorber design and customized chirped fiber Bragg grating (CFBG) need to match the gain medium of the fiber laser. The NOLM with an eight-figure cavity could be operated at significant mechanical vibration, but the relatively long cavity length restricts its repetition rate. The NPE mode-locking does not require any additional modulator, it can directly generate a short pulse of sub 7-cycle and high repetition rate of 750 MHz.[19,20]

In this paper, we present an f_0-stabilized Yb-fiber frequency comb based on an NPE mode-locked laser oscillator and study the pump-induced f_0 dynamics. A nonlinear f_0 variation with wide dynamic range over 200 MHz is observed. Through the passive stabilization of the f_0 signal and feedback controlling the pump power by a self-made PLL electronics, an uninterrupted phase-locking is achieved with a residual frequency jitter of 85 mHz in 1-hour accumulation time.

2. Experimental setup

The f_0 stabilization of the Yb-doped fiber frequency comb is schematically illustrated in Fig. 1. It is composed of an NPE mode-locked Yb-doped fiber oscillator, Yb-doped fiber amplifier (YDFA), pulse compressor, f–$2f$ interferometer, and locking electronics. The oscillator is built with a unidirectional ring cavity, where a 70-cm Yb-doped single-mode fiber (OFS,Yb350) is used as the gain medium. The free-space section consists of a polarization-dependent isolator (ISO) that ensures the unidirectional operation, a polarization beam splitter (PBS) for the pulse rejection, and a pair of double-pass reflective gratings (600 lines/mm groove density) providing negative group-delay dispersion to compensate for the fiber dis-

*Project supported by the National Natural Science Foundation of China (Grant No. 11274115), the National Key Project for Basic Research, China (Grant No. 2011CB808105), and the National Key Scientific Instrument Project, China (Grant No. 2012YQ150092).

†Corresponding author. E-mail: wxli@phy.ecnu.edu.cn

© 2014 Chinese Physical Society and IOP Publishing Ltd

persion inside the cavity. The semi-fiber and semi-free space are connected by a pair of collimators (Cols). The polarization state of the pulse is controlled by two quarter-wave-plates (QWPs) and a half-wave-plate (HWP), and mode-locking is launched through carefully rotating the three waveplates. The output pulse train is then amplified by an all-fiber pre-amplifier and a main amplifier. The gain medium of the main amplifier is a 1.0-m-long double-clad large-mode-area polarization-maintaining photonic crystal fiber (LMA Yb-PCF), which has a core diameter of 40 μm. It is end-pumped in free space by high-power laser diodes at 976 nm. The chirped pulses are amplified to output an average power of 5 W, and then compressed by two volume holographic transmission gratings (1250 lines/mm groove density)

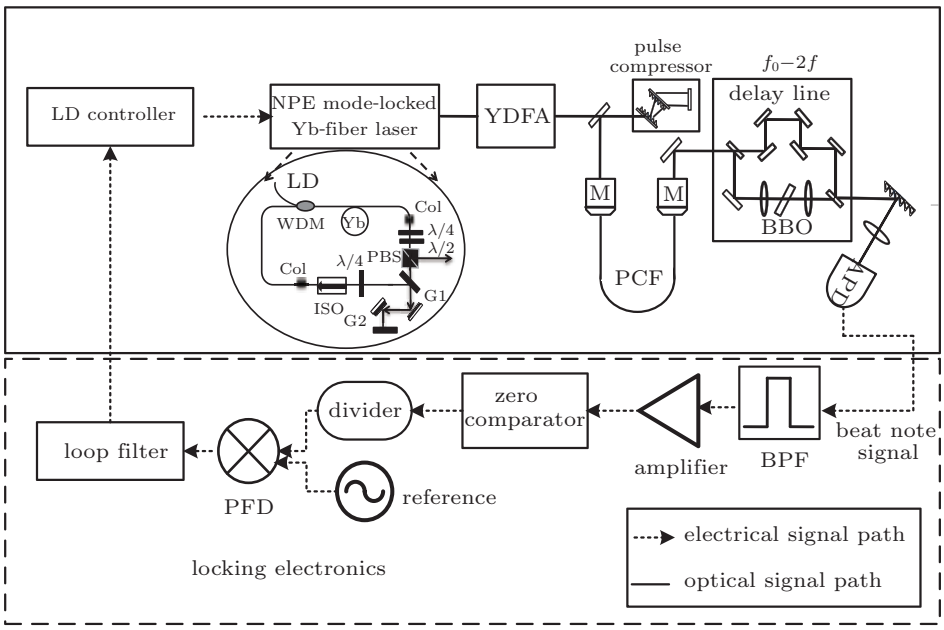


Fig. 1. Schematic illustration of the f_0 stabilization of the Yb-fiber frequency comb. NPE: nonlinear-polarization-evolution; LD: laser diode; WDM: wavelength-division multiplexing; Yb: Yb-doped single-mode fiber; Col: collimator; λ/4: quarter-wave plate; λ/2: half-wave plate; ISO: optical isolator; G1, G2: grating pair; PBS: polarization beam splitter; YDFA: Yb-doped fiber amplifier; M: micro-objective lens; PCF: photonic crystal fiber; BBO: beta-barium borate crystal; APD: avalanche photodiode; BPF: band-pass filter; PFD: phase-frequency detector.

The compressed pulse train is then sent to the self-referenced f_0–2f interferometer to extract the f_0 signal. The octave supercontinuum is generated from a 20-cm photonic crystal fiber (PCF) with a zero dispersion wavelength of 890 nm. The part of long-wavelength side is frequency-doubled by a beta-barium borate crystal (BBO) and part of short-wavelength is delayed through a time-delay line. The overlapped signal is detected by an avalanche photodetector (APD210, Menlo Systems) for beat signal detection.

In the phase-lock loop (PLL) electronics, the f_0 is first filtered out by a 20-MHz band-pass filter (BPF), and then amplified with a high-gain RF amplifier. After the zero comparator (AD8861), the analog signal is transformed into a digital one. In terms of the Yb-fiber laser response, the feedback bandwidth typically ranges from 5 kHz to 15 kHz.[21] In order to expand the locking range, the digitalized signal is subsequently lowered down by a factor of 64 using a high-speed frequency divider (74HC4040). The referenced frequency standard is a 312.5-kHz square wave from an arbitrary signal generator (Tektronix AFG3252), which is governed by an Rb-microwave clock. Although the frequency mixer has prominent advantages in less residual noise, it lacks robustness and reliability to lock f_0 as a limited capture range.[22] In our scheme, the frequency difference between the divided f_0 and the local reference is compared by a phase-frequency detector (PFD, AD9901). It has a dynamic range from $-\pi$ to π. The output from AD9901 is a pulse train with variable duty cycle indicating the phase error. The phase error signal is low-pass filtered by a loop filter, and sent to drive the auxiliary modulation port of the LD controller (ILX 3565) with a modulation rate of 200 mA/V.

3. Results and discussion

The distance of the grating is tuned to $\sim$ 60 mm where the shortest pulse is compressible to 58 fs, which implies that the oscillator operates in the near zero net-cavity dispersion regime.[23] The oscillator spectrum is centered at $\sim$ 1030 nm with a bandwidth of 45 nm. After amplification, the output spectrum is influenced by the gain narrowing. The bandwidth

is reduced to 10 nm as shown in Fig. 2(a). The amplified pulse is then dechirped by using pulse compressor, generating femtosecond pulses of 191 fs in duration, fitted by Gaussian profile. The corresponding autocorrelation trace is shown in Fig. 2(b).

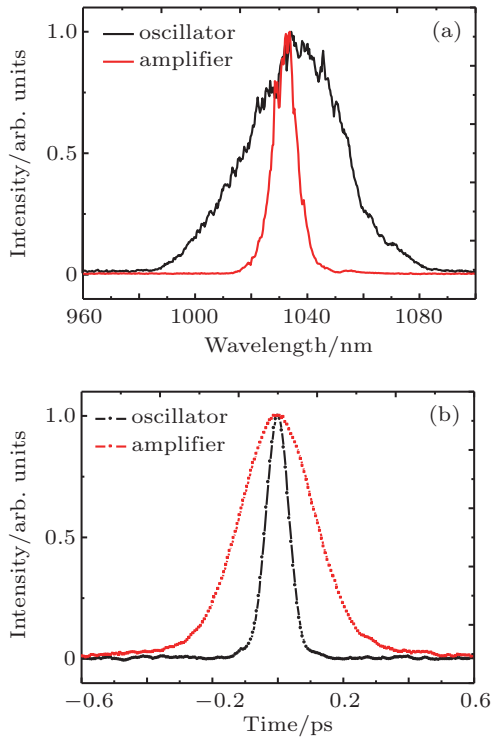


Fig. 2. (color online) (a) Output optical spectrum of the oscillator and amplifier. (b) The measured autocorrelation traces of the compressed pulses from the oscillator and amplifier respectively.

The compressed pulse train with an average power of 500 mW is coupled into the PCF by a micro-objective lens, corresponding to an input energy of ~ 8 nJ. After adjusting the polarization of the input pulse, the broadband spectrum spanning from 600 nm to 1300 nm could be observed [Fig. 3(a)]. Two peaks at 610 nm and 1220 nm are picked out for the f_0–$2f$ detection. When the temporal and spatial overlaps of the two branches are well-adjusted, the free-running f-related beat-signal can be observed in a 100-kHz resolution bandwidth (RBW) with an RF spectrum analyzer [Fig. 3(b)]. It mixes the harmonics of repetition rate (f_r) with other frequency components relative to f_0. The fundamental frequency of f_r is 60 MHz, which is dependent on the cavity length of the oscillator. The noise floor on the beat signal shows the evidence of excess noise during supercontinuum generation.

The f_0 could be shifted by changing the pump power of the oscillator. The response of f_0 to the pump current is illustrated in Fig. 4(a), indicating the f_0 has a dynamic range over 200 MHz as the pump current increases from 90 mA to 200 mA. It is worth noticing that the f_0 tuning curve is nonlinear. The slope of f_0 gradually lowers down as the pump current increases, which is similar to the result of the Ti:sapphire comb observed by Holman *et al.*[24] and the result of the Er:Yb:glass-based frequency comb obtained by Bucalovic *et al.*[25] However, in contrast to the reversal points found in those two experiments,[24,25] the f_0 change is monotonic in our comb.

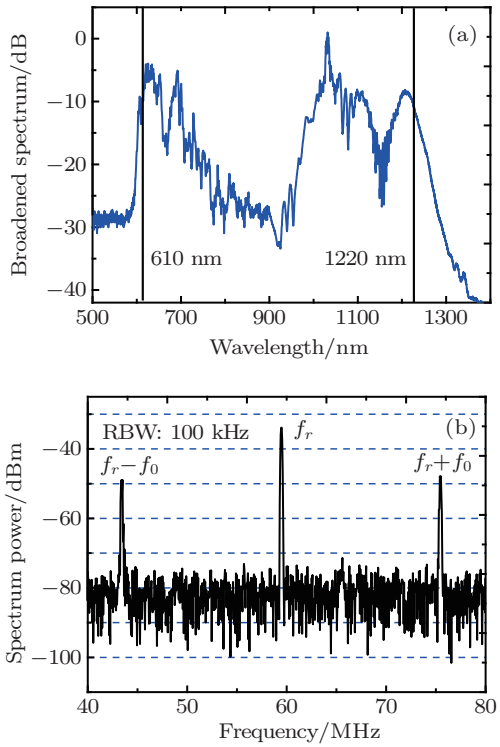


Fig. 3. (color online) (a) Supercontinuum generated in the PCF with the black lines showing the spectrum peaks at 610 nm and 1220 nm for heterodyne note. (b) The detected beat signal in an RBW of 100 kHz.

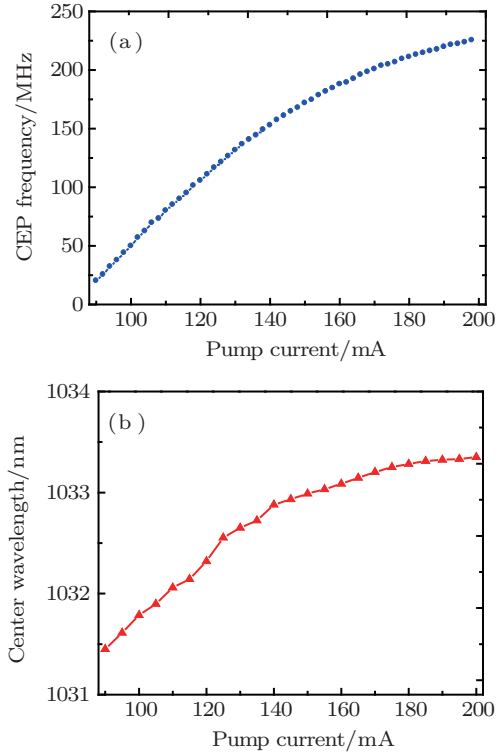


Fig. 4. (color online) (a) Response of f_0 to pump current, and (b) central wavelength of the oscillator spectrum varying with pump current.

The pump-induced change in f_0 can be explained by the spectral shift of the mode-locked fiber laser.[26] In the mode-locked fiber laser system, the pump power change produces a perturbation on the steady-state running. The perturbation mainly includes self-phase modulation (SPM) and pump-induced spectral shift. The SPM directly leads to a nonlinear carrier phase and sets an intercept, while the pump-induced spectral shift affects the arrival time of the pulse envelope in a round trip and determines the slope. Through the optical spectrum analyzer (Yokogawa AQ6370) with a high resolution of 0.02 nm, the centers of the spectrum at different pump powers are recorded. As shown in Fig. 4(b), the central wavelength is red-shifted with the increase of pump power. The shift is saturated at high pump power. This is limited by the gain bandwidth of Yb^{3+}.

According to the theory given by Washburn *et al.*,[26] pump-induced f_0 change is dominated by the spectral shift, which can be expressed as[26]

$$\frac{\mathrm{d}f_0}{\mathrm{d}P} = \frac{f_r}{2\pi}\frac{\mathrm{d}\varphi_{\mathrm{SPM}}}{\mathrm{d}P} - \frac{\beta_0\beta_2 f_r^2}{2\pi}\frac{\mathrm{d}\omega_\Delta}{\mathrm{d}P},$$

where β_0 and β_2 are the n-th order propagation constant, and ω_Δ is the pump-induced central frequency shift. For our frequency comb, the calculated intercept induced is about 0.5 MHz/mA. Combined with the measured center spectral values in Fig. 4(b), the overall pump-induced f_0 change $\mathrm{d}f_0/\mathrm{d}I_\mathrm{P}$ is given in Fig. 5 (solid line). The blank circles show the measured values of $\mathrm{d}f_0/\mathrm{d}I_\mathrm{P}$, which are taken from the derivative of the polynomial fit to the data shown in Fig. 4(a). They are in good agreement except for the two ends. The deviations at the curve ends in Fig. 5 are due to other nonlinear factors such as third-order dispersion and resonant group velocity.[26]

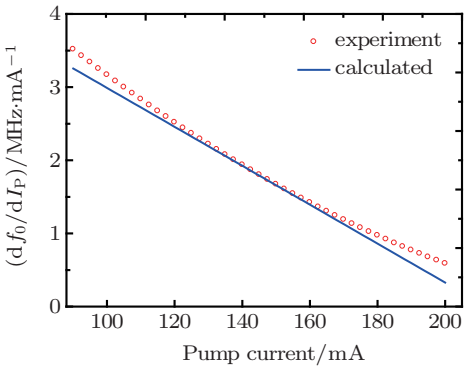


Fig. 5. (color online) Measured (blank circle) and calculated (solid line) values of pump-induced f_0 change $\mathrm{d}f_0/\mathrm{d}I_\mathrm{P}$ varying with pump current.

In an NPE mode-locked laser oscillator, the intra-cavity polarization state is subjected to random change caused by the fiber birefringence under environmental disturbance. This usually affects mode-locking status and the stability of the f_0. We conducted several schemes to reduce the undesired effect. Firstly the fiber is glued on the breadboard and the oscillator is enclosed with an inch-thick aluminium sheet to isolate from air flows.

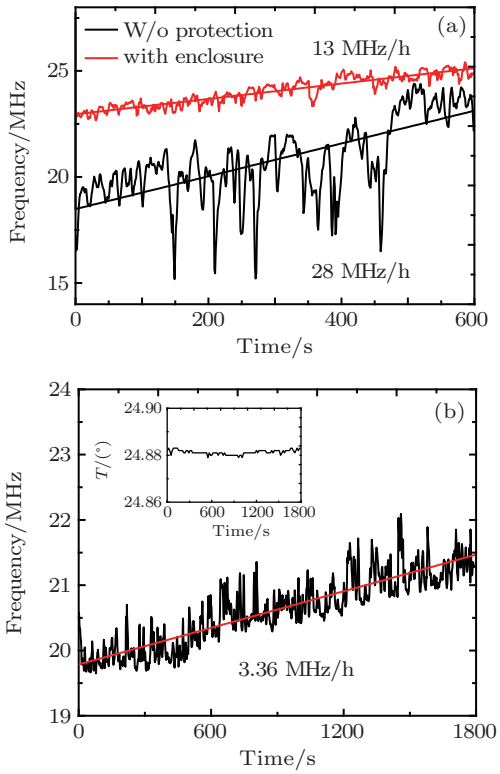


Fig. 6. (color online) (a) Frequency drifts of f_0 without any protection and with enclosure, and (b) frequency drift of f_0 with temperature control for the pump diode. Inset shows the recorded temperature variation of the pump diode with time.

Figure 6(a) shows the fluctuation of f_0 in the absence of external control. The f_0 drift rate is 28 MHz per hour and severely fluctuates with some sudden shifts over 5 MHz, which are reduced to 13 MHz per hour with the above-mentioned enclosure. The operating temperature of the pumping laser diode for oscillator is another significant factor responsible for the drift of f_0. The pumping power fluctuation results from the environmental temperature variation-produced additional instability of f_0. A thermal electronic cooler (TEC) is employed to precisely control the operation temperature of the pump diode, which is kept constantly at 24.88 °C with a standard deviation of 0.0095 °C within half an hour. In such a case, the accumulated frequency drift is 1.68 MHz in half an hour as presented in Fig. 6(b). The observed spikes result from the random acoustic vibration.

After adding another layer of lead-foam pad to package the oscillator, the acoustic vibration is well attenuated. The amplitudes of the spikes decrease below 0.5 MHz and the drift is less than 3 MHz within an hour as shown in Fig. 7(a). As the pump diode current varies linearly with pump power, the direct control of the injection current is implemented to stabilize f_0. Feedback controlling the pump current through the PLL

electronics, the recorded f_0 frequency fluctuation is given in Fig. 7(b). The central frequency is 20 MHz and the standard deviation is 85 mHz. Compared with the results reported in Refs. [27] and [28], the relatively low frequency accuracy is affected mainly by the limited signal-to-noise (SNR) of f_0.

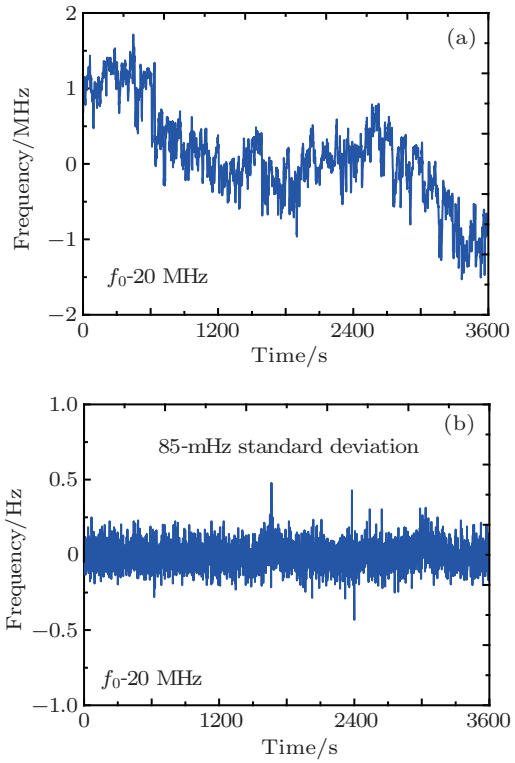


Fig. 7. (color online) (a) Recorded frequency counter of f_0 in the free-running condition with acoustic vibration attenuation, and (b) phase-locked f_0 within 1 hour.

4. Conclusions

In this paper, we have phase-stabilized the carrier envelope offset frequency of an Yb-doped optical frequency comb through feedback control of the current of pump laser diode. The relationship between the pump-induced f_0 dynamics and the related spectrum shift is confirmed. Through reducing the environmental noise, the stability of the free-running carrier envelope offset frequency has a ~ 10 folder improvement. Further phase-stabilized f_0 signal with a frequency jitter of 85 mHz within 1 hour is achieved with PLL electronics. Such a frequency comb would be an important tool for generating the XUV frequency comb or the Ca-ion optical clock.

References

[1] Zhang J T, Wu X J, Li Y and Wei H Y 2012 *Acta Phys. Sin.* **61** 100601 (in Chinese)
[2] Cao S Y, Cai Y, Wang G Z, Meng F, Zhang Z G, Fang Z J and Li T C 2011 *Acta Phys. Sin.* **60** 094208 (in Chinese)
[3] Diddams S A 2010 *J. Opt. Soc. Am. B* **27** B51
[4] Han H N, Zhang W, Wang P, Li D H, Wei Z Y, Shen N C, Nie Y X, Gao Y P, Zhang S G and Li S Q 2007 *Acta Phys. Sin.* **56** 2760 (in Chinese)
[5] Zhao J, Li W, Bai D, Yang K, Ru Q, Liu Y, Li L and Zeng H 2013 *Laser Phys.* **23** 095112
[6] Klenner A, Golling M and Keller U 2013 *Opt. Express* **21** 10351
[7] Baumann E, Giorgetta F R, Nicholson J W, Swann W C, Coddington I and Newbury N R 2009 *Opt. Lett.* **34** 638
[8] Wilken T, Lezius M, Hänsch T W, Kohfeldt A, Wicht A, Schkolnik V, Krutzik M, Duncker H, Hellmig O, Windpassinger P, Sengstock K, Peters A and Holzwarth R 2013 *CLEO: Applications and Technology, June 9–14, San Jose, California, USA*, AF2H.5
[9] Ruehl A 2012 *Optics and Photonics News* **23** 30
[10] Li W, Hao Q, Yan M and Zeng H 2009 *Opt. Express* **17** 10113
[11] Li W, Yang K, Yan M, Zhou H, Ding J and Zeng H 2011 *Laser Phys.* **21** 531
[12] Yang K, Li W, Yan M, Shen X, Zhao J and Zeng H 2012 *Opt. Express* **20** 12899
[13] Pupeza I, Holzberger S, Eidam T, Carstens H and Pupeza I 2013 *Nat. Photon.* **7** 608
[14] Yasuda M, Kohno T, Inaba H, Nakajima Y, Hosaka K, Onae A and Hong F 2010 *J. Opt. Soc. Am. B* **2** 7
[15] Gill P 2011 *Philost. R. Soc. A* **369** 4109
[16] Washburn B R, Diddams S A and Newbury N R 2004 *Opt. Lett.* **29** 250
[17] Xia H, Zhang X and Li H 2014 *Chin. Phys. B* **23** 024209
[18] Pal P, Knox W H, Hartl I and Fermann M E 2007 *Opt. Express* **15** 12161
[19] Kurita T, Yoshida H, Kawashima T and Miyanaga N 2012 *Opt. Lett.* **37** 3972
[20] Li C, Wang G, Jiang T, Wang A and Zhang Z 2013 *Opt. Lett.* **38** 314
[21] Peng J L, Ahn H, Shu R H, Chui H C and Nicholson J W 2007 *Appl. Phys. B* **86** 1
[22] Wang X L, Tao T J Wu B, Xu Y F, Wang Z Y and Lin Q 2011 *Chin. Phys. Lett.* **28** 084214
[23] Yan M, Li W, Yang K, Zhou H, Shen X, Zhou Q, Ru Q, Bai D and Zeng H 2012 *Opt. Lett.* **37** 1511
[24] Holman K W, Jones R J, Marian A, Cundiff S T and Ye J 2003 *IEEE J. Sel. Top. Quant.* **9** 1018
[25] Bucalovic N, Dolgovskiy V, Schori C, Domenico G D, Keller U, Schilt S and Südmeyer T 2012 *Opt. Lett.* **37** 4428
[26] Washburn B R, Swann W C and Newbury N R 2005 *Opt. Express* **13** 10622
[27] Schibli T R, Hartl I, Yost D C, Martin M J, Marcinkevicius A, Fermann M E and Ye J 2008 *Nat. Photon.* **2** 355
[28] Kim Y, Kim S, Kim Y, Hussein H and Kim S W 2009 *Opt. Express* **17** 11972